# Absorption Spectra of Solids from Periodic Equation-of-Motion Coupled-Cluster Theory

Xiao Wang<sup>1</sup> and Timothy C. Berkelbach<sup>1,2,\*</sup>

<sup>1</sup>Center for Computational Quantum Physics, Flatiron Institute, New York, New York 10010 USA <sup>2</sup>Department of Chemistry, Columbia University, New York, New York 10027 USA

We present ab initio absorption spectra of six three-dimensional semiconductors and insulators calculated using Gaussian-based periodic equation-of-motion coupled-cluster theory with single and double excitations (EOM-CCSD). The spectra are calculated efficiently by solving a system of linear equations at each frequency, giving access to an energy range of tens of eV without explicit enumeration of excited states. We assess the impact of cost-saving approximations associated with Brillouin zone sampling, frozen orbitals, and the partitioned EOM-CCSD approximation. Although our most converged spectra exhibit lineshapes that are in good agreement with experiment, they are uniformly shifted to higher energies by about 1 eV, which is not explained by the remaining finite-size errors. We tentatively attribute this discrepancy to a combination of vibrational effects and the remaining electron correlation, i.e., triple excitations and above.

#### I. INTRODUCTION

Absorption spectroscopy is an important tool for studying the electronic properties of materials. For semiconductors and insulators, the low energy part of the absorption spectrum is typically dominated by excitonic effects, which originate from electron-hole interactions that may be screened by the other electrons. The most common computational methods currently used for simulating absorption spectra are timedependent density functional theory (TDDFT) [1-3] and the Bethe-Salpeter equation based on the GW approximation to the self-energy (GW-BSE) [4-8]. In TDDFT, it has long been recognized that the inclusion of nonlocal exchange is critical for the description of excitons [9–12], and promising recent work has applied screened or dielectric-dependent range-separated hybrids [13, 14]. The GW-BSE approach is based on time-dependent many-body perturbation theory and typically includes screening at the level of the randomphase approximation. The predictions are reasonably accurate when compared to experiments, although implementation details, starting point dependence, and the absence of finite-temperature or vibrational effects make a rigorous evaluation challenging. For example, benchmark studies on molecules [15-18] have found that the GW-BSE results depend strongly on the reference functional and the optimal functionals are very different than those typically used for solid-state calculations.

Recent years have seen rapid development of wavefunction-based quantum chemistry techniques for periodic solids [19–25]. In the present context of neutral excitation energies, equation-of-motion coupled-cluster theory with single and double excitations (EOM-CCSD) is a promising alternative to TDDFT or GW-BSE. For example, our group has applied EOM-CCSD to study plasmons in models of metals [26, 27], as well as singly- and doubly-excited states in a molecular crystal [28]. Recently, the two of us presented a systematic study of EOM-CCSD for a range of semiconductors and insulators, finding an accuracy of about 0.3 eV for the first singlet excitation energy [29]. Although these preliminary results are

encouraging, the optical response of solids is encoded in the full energy-dependent absorption spectrum, which depends on all excited states in the energy range of interest and their oscillator strengths. Here, we extend our previous work and study the absorption spectra of semiconductors and insulators predicted by EOM-CCSD.

The remainder of the paper is organized as follows. In Sec. II, we briefly describe the theory underlying the calculation of solid-state absorption spectra with periodic EOM-CCSD. In Sec. III, we provide computational details about the basis sets used, integral evaluation, and *k*-point sampling. In Sec. IV, we first present and discuss our final EOM-CCSD optical absorption spectra for six solids, before demonstrating detailed studies of the impact of various approximations. Finally, in Sec, V, we summarize our results and conclude with future directions.

#### II. THEORY

Within EOM-CC theory [30–36], excited states are found given by

$$|\Psi_n\rangle = \hat{R}_n e^{\hat{T}} |\Phi_0\rangle \tag{1}$$

where  $\hat{T}$  and  $\hat{R}_n$  create particle-hole excitations. The  $\hat{T}$  operator is determined by the solution of the nonlinear CC amplitude equations and the  $\hat{R}_n$  operator is determined by a non-Hermitian matrix eigenvalue problem. Within the CC framework, the polarization-averaged absorption spectrum at frequency  $\omega$  is  $I(\omega) = \sum_{\mathcal{E}=(x,y,z)} I_{\mathcal{E}}(\omega)$ , where

$$I_{\xi}(\omega) = \frac{1}{\omega^2} \sum_{n>0} \langle \tilde{\Psi}_0 | \hat{p}_{\xi} | \Psi_n \rangle \langle \tilde{\Psi}_n | \hat{p}_{\xi} | \Psi_0 \rangle \delta(\omega - (E_n - E_0)), \quad (2)$$

 $\Psi_0$  ( $\tilde{\Psi}_0$ ) is the right-hand (left-hand) CC ground-state wavefunction with energy  $E_0$ ,  $\Psi_n$  ( $\tilde{\Psi}_n$ ) is the right-hand (left-hand) CC excited-state wavefunction with energy  $E_n$ , and  $\hat{p}_{\xi}$  is the momentum operator in the  $\xi$  direction. Note that we work in the velocity gauge as appropriate for periodic systems and divide by  $\omega^2$  to approximate the imaginary part of the dielectric function [7].

<sup>\*</sup> tim.berkelbach@gmail.com

In crystals, the density of excited states prohibits their direct enumeration. Instead we calculate  $I_{\xi}(\omega)$  using the correction vector method [26, 37–39]

$$I_{\xi}(\omega) = -\frac{1}{\pi\omega^2} \operatorname{Im}\langle \tilde{\Psi}_0 | \hat{p}_{\xi} [\omega - (\hat{H} - E_0) + i\eta]^{-1} \hat{p}_{\xi} | \Psi_0 \rangle, \quad (3)$$

where  $\eta$  is a numerical Lorentzian linewidth, which can be checked by inserting a resolution of the identity,  $1 = \sum_n |\Psi_n\rangle \langle \tilde{\Psi}_n|$ . After replacing the right- and left-hand ground-state wavefunctions with their CC expressions  $|\Psi_0\rangle = e^{\hat{T}} |\Phi_0\rangle$ ,  $\langle \tilde{\Psi}_0| = \langle \Phi_0| (1 + \hat{\Lambda}) e^{-\hat{T}}$  where  $\hat{\Lambda}$  is the deexcitation operator in CC theory, we arrive at the final expression

$$I_{\xi}(\omega) = -\frac{1}{\pi\omega^2} \text{Im}\langle \Phi_0 | (1 + \hat{\Lambda}) \hat{\bar{p}}_{\xi} | x_{\xi}(\omega) \rangle$$
 (4a)

$$[\omega - (\hat{\bar{H}} - E_0) + i\eta] |x_{\xi}(\omega)\rangle = \hat{\bar{p}}_{\xi} |\Phi_0\rangle. \tag{4b}$$

where  $\hat{O} = e^{-\hat{T}}\hat{O}e^{\hat{T}}$  are similarity-transformed operators. Projecting Eq. (4b) into a basis of excited determinants yields a system of linear equations for the correction vector  $\mathbf{x}_{\xi}(\omega)$  that can be solved by iterative techniques; here, we use the two-parameter generalized conjugate residual method with implicit inner orthogonalization [40] as implemented in SciPy [41]. This system of linear equations can be solved independently at each frequency in order to construct the spectrum without explicit enumeration of excited states.

Here, we study the performance of EOM-CC with single and double excitations (EOM-CCSD), i.e.  $\hat{T} = \hat{T}_1 + \hat{T}_2$ ,  $\hat{\Lambda} = \hat{\Lambda}_1 + \hat{\Lambda}_2$ , and  $\hat{R} = \hat{R}_1 + \hat{R}_2$ . For each frequency  $\omega$ , the cost of iteratively solving the system of linear equations (4b) scales as  $O(N_k^4 N_o^2 N_v^4)$ , where  $N_k$  is the number of k-points sampled in the Brillouin zone and  $N_o, N_v$  are the number of occupied and virtual orbitals in the unit cell. The number of iterations required depends on several technical details, including the initial guess, the diagonal preconditioner, and the linewidth  $\eta$ . Convergence is easier for larger values of  $\eta$ ; for the values used here, we typically converge to graphical accuracy within 3-5 outer iterations (hundreds of matrix-vector products) for small values of  $\omega$ . However, for large values of  $\omega$ , the convergence becomes slower and frequently needs 10 or more iterations to converge. Therefore, in this work we also test and apply so-called partitioned EOM-CCSD [42–44], where the double excitation block of the similarity transformed Hamiltonian is approximated by a diagonal matrix of orbital energy differences. This reduces the iterative scaling of the EOM step to  $O(N_k^3 N_q^2 N_v^3)$ . This approximation corresponds to a truncated, low-order treatment of screening, which was recently found to work well for band gaps [45], although its accuracy degrades for small-gap semiconductors.

As an alternative to EOM-CC, one can use the linearresponse coupled cluster (LR-CC) theory to calculate excitedstate properties. When no truncation is carried out in the excitation levels, LR-CC and EOM-CC both give exact results. At a truncated excitation level, the methods yield identical excitation energies but different excited-state properties, such as transition dipole moments, and only properties predicted by LR-CC are properly size extensive [46, 47]. Although this finding calls into question the applicability of EOM-CCSD for solid-state absorption spectra, the violation of size extensivity is strongly mitigated when large basis sets are used [48]. In this work, we observe no problems associated with this deficiency of EOM-CCSD for spectra, perhaps because of the near completeness of the basis set in periodic solids.

#### III. COMPUTATIONAL DETAILS

All calculations were performed with PySCF [49, 50]. The relatively high cost of periodic CCSD calculations makes it challenging to achieve convergence to the complete basis set and thermodynamic limits. We have tested convergence with respect to Brillouin zone sampling, basis sets, frozen orbitals, and the partioned EOM approximation, which will be analyzed in detail in Sec. IV B. Based on our studies, our spectra presented in Sec. IV A are performed in the following way. We use GTH pseudopotentials [51, 52] and the corresponding polarized double-zeta basis set (DZVP) [53]. Two-electron repulsion integrals were treated by periodic Gaussian density fitting with an even-tempered auxiliary basis [54]. In the CCSD calculations, we correlate the highest four occupied and the lowest four virtual orbitals at each k-point, while all of the other orbitals are frozen. The partitioning approximation is made to the similarity transformed Hamiltonian whereby the dense doubles block is replaced by a diagonal matrix of orbital energy differences [42–44]. The Brillouin zone was sampled with a uniform mesh of up to  $N_k = 5 \times 5 \times 5$  k-points. The k-point mesh is shifted to include either the  $\Gamma$  point or the random symmetry-breaking point k = (0.11, 0.21, 0.31) (in fractions of the reciprocal lattice vectors). Such random shifts have been previously shown to yield absorption spectra that converge more quickly to the thermodynamic limit [55]. We then calculate the necessary correction to the first excitation energy due to finite-site effects, frozen orbitals, and the partitioning approximation. Finally, we rigidly shift the entire absorption spectrum by this correction, which has a magnitude of 0.1–0.6 eV for the materials and k-point meshes considered

#### IV. RESULTS AND DISCUSSION

In Sec. IV A, we present and analyze our best and final absorption spectra of six solids, calculated using the approximations and corrections discussed above and analyzed in detail in Sec. IV B. We refer to these results as those predicted by "EOM-CCSD" for notational simplicity and because the corrections are designed to yield EOM-CCSD results, but we emphasize that some errors remain with respect to exact EOM-CCSD results.

## A. EOM-CCSD absorption spectrum for six solids

In Fig. 1, we show the approximate EOM-CCSD absorption spectra (see Secs. III and IVB for approximation details and analysis) of six three-dimensional semiconducting

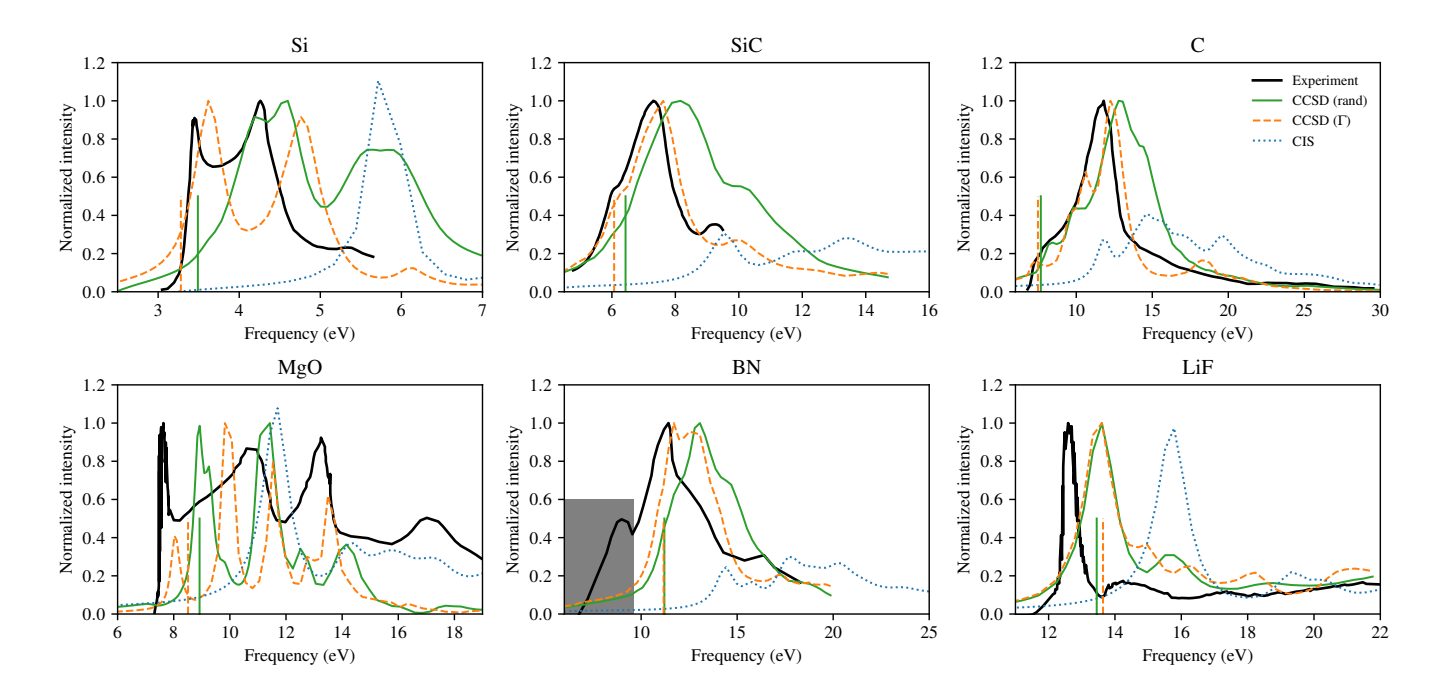


FIG. 1. Absorption spectra of Si, SiC, C, MgO, BN, and LiF in the DZVP basis set. A  $5 \times 5 \times 5$  k-point mesh is used for all CCSD spectra (green and orange) and a  $7 \times 7 \times 7$  k-point mesh for all CIS spectra (blue). CCSD spectra are obtained from partitioned EOM-CCSD with the highest 4 occupied and the lowest 4 virtual orbitals correlated at each k-point and then rigidly shifted, as described in Sec. IV B. For each solid, two CCSD spectra are shown with k-point meshes that are shifted to include a random, symmetry-breaking k-point (solid green) or the  $\Gamma$  point (dashed orange). The corresponding EOM-CCSD first excitation energies are indicated by green and orange vertical lines. Each CIS spectrum is scaled by the same amount as the corresponding EOM-CCSD spectrum (with random k-point shift) to facilitate comparison of their intensities. A broadening of  $\eta = 0.5$  eV is used in all calculations except for silicon where a smaller broadening of  $\eta = 0.2$  eV is used to resolve the sharper peaks. The calculated spectra are compared to the experimental data (thick black) of Si [56], SiC [57], C [58], MgO [59], BN [60], and LiF [59]. For BN, the shaded region of the experimental spectrum should be ignored as it has been attributed to defects and polymorphism [61].

and insulating materials: Si, SiC, C, MgO, BN, and LiF. The experimental lattice constants were used for all systems: Si (5.431 Å), SiC (4.350 Å), C (3.567 Å), MgO (4.213 Å), BN (3.615 Å), and LiF (4.035 Å). Spectra were obtained using a  $5\times5\times5$  k-point mesh; in order to give some sense of remaining finite-size errors, we show EOM-CCSD results obtained with the two k-point shifts mentioned above. Our EOM-CCSD absorption spectra are compared to experimental ones and to those obtained by configuration interaction with single excitations (CIS), which was performed with a denser  $7 \times 7 \times 7$  k-point mesh.

As seen in Fig. 1, the EOM-CCSD spectra are in reasonably good agreement with experiment. For large gap insulators (like BN and LiF), the two k-point shifts give similar spectra, indicating that the remaining finite-size errors are small. In contrast, for small gap semiconductors (like Si and SiC), the two k-point shifts give different spectra, indicating that the remaining finite-size errors of at least one of the spectra are large. Based on the results in Sec. IV B, we believe that the randomly shifted k-point mesh yields spectra that are closer to the thermodynamic limit. Comparing results obtained with the randomly-shifted k-point mesh to experiment, we see that EOM-CCSD spectra are shifted to higher energies by about 1 eV, but otherwise have very similar lineshapes, indicating an accurate description of excitonic interactions and concomitant

redistribution of spectral weight. By comparison, CIS spectra massively overestimate the excitation energies of solids by 3 eV or more, as shown in our previous work [29], and often have qualitatively incorrect spectral structure. Because Hartree-Fock-based CIS is identical to unscreened GW-BSE, these results emphasize the well-known importance of screening, especially in semiconductors.

We believe that the shift to higher energies that is exhibited by EOM-CCSD when compared to experiment is mostly attributable to the missing correlation due to the neglect of triple (and higher) excitations and the absence of vibrational and finite-temperature effects, which are of course present in experiments and absent in the calculations. However, it is hard to rule out finite-size errors, especially for small gap semiconductors like Si or SiC. With regards to electron correlation, it is interesting to note that our previous work, which did not study spectra, found that EOM-CCSD overestimated the first excitation energy by about 0.3 eV, which is noticably smaller than the deviations seen in the spectra in Fig. 1. This discrepancy (i.e. overestimation by 0.3 eV versus 1 eV or more) is because the first excited state, especially in indirect gap materials, is typically weakly absorbing and contributes to the gradual onset of absorption. However, experimentally reported first excitation energies are typically those of spectral peaks or intense features, which occur at higher energies than

the onset of absorption. In Fig. 1, the vertical lines indicate the calculated first excitation energies, which are corrected for finite-size effects and other approximations mentioned in Sec. III.

In contrast to the apparent differences in spectra, the use of differently shifted k-point meshes produce first excitation energies that agree reasonably well with each other, with a difference of 0.04–0.4 eV. The first excitation energies differ from our previously reported values [29] (by 0.2 eV or less) due to a slightly different treatment of the finite-size effects in the current work, i.e. (a) we extrapolate the data using a function of the form  $E_{\infty} + aN_k^{-1}$ , (b) here, the  $5 \times 5 \times 5$  result is included in extrapolation, and (c) the partitioning approximation is corrected by a constant shift deduced from the  $3 \times 3 \times 3$ result. Naturally, we believe that the comparison of spectra, as done here, enables the most fair evaluation of the accuracy. However, this overestimation of excited states by 1 eV or more is significantly higher than the known performance of EOM-CCSD in molecules. This difference is surprising, especially given that the excitonic states contributing to absorption are all predominantly single-excitation in character and that the EOM-CCSD polarizability has most of the diagrammatic content of the GW-BSE polarizability, plus more [26, 28, 62, 63].

The worst agreement between EOM-CCSD and experiment is for silicon, which has the smallest gap of all materials considered. In its experimental spectrum, the main features are the two peaks at 3.5 eV and 4.3 eV with similar intensity. While EOM-CCSD predicts a first excitation energy of about 3.5 eV, this state has a low spectral intensity. The two spectral peaks appear at 4.1 and 4.6 eV (randomly shifted) or 3.6 and 4.9 eV ( $\Gamma$ -centered). In addition to vibrational effects, we believe that the poor agreement between theory and experiment is due to the large remaining finite-size errors and the errors associated with the partitioning approximation, both of which are expected to be largest for this small-gap semiconductor.

#### B. Approximations and error corrections

Finite-size errors of excited-state properties like absorption spectra have been widely discussed in the TDDFT and GW-BSE literature [7, 13, 64–66], in part due to the relative maturity and low computational cost of these methods. In constract, the finite-size errors of wavefunction-based methods such as CCSD have been studied signficantly less, especially for spectra. In the following, we will use diamond as an example to study the finite-size errors of the spectra predicted by the EOM-CCSD.

As a warm-up to EOM-CCSD, we first consider CIS, which forms a minimal theory for electronic excited states in the condensed phase and is qualitatively comparable to TDDFT and GW-BSE. Importantly, the relatively low cost of CIS allows us to study the convergence with respect to Brillouin zone sampling up to relatively large k-point meshes. In the upper panels of Fig. 2, we show the CIS absorption spectra computed with various k-point meshes centered at  $\Gamma$  (right column) or randomly shifted (left column), including up to  $7 \times 7 \times 7$  k-point meshes. At low mesh densities (like  $3 \times 3 \times 3$ ), the spectra

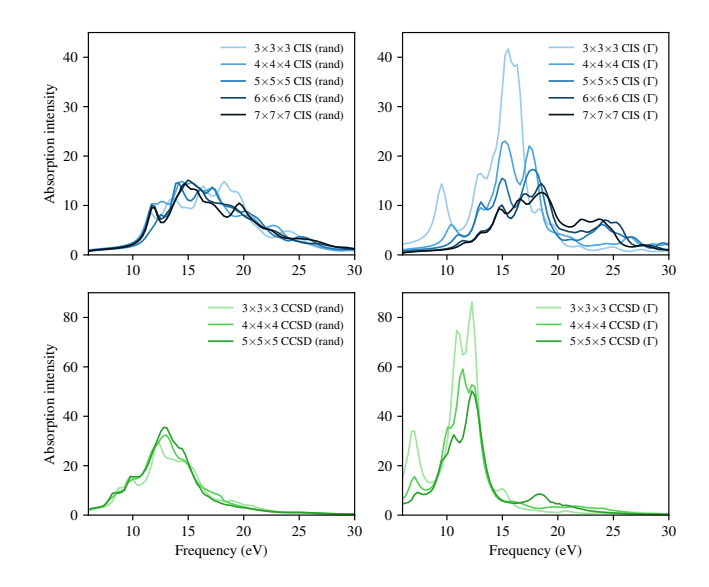


FIG. 2. Convergence of the CIS (top) and EOM-CCSD (bottom) spectra of diamond using various k-point shifts and sampling densities. A Lorentzian broadening of  $\eta = 0.5$  eV is used in all cases.

computed with different k-point shifts show a large discrepancy in both peak positions and intensities. This discrepancy is due to insufficient Brillouin zone sampling and largely depends on details of the band structure. As the mesh density is increased, the spectra converge to a similar result, but the convergence is much more rapid with the randomly shifted k-point mesh. Even for this insulator, the CIS spectra are not graphically converged with a  $7 \times 7 \times 7$  mesh. This must be kept in mind when analyzing the EOM-CCSD spectra in Fig. 1, which are limited to  $5 \times 5 \times 5$  meshes.

In the lower panels of Fig. 2, the EOM-CCSD spectra of diamond with the same two k-point shifts are shown, for mesh densities ranging from  $3 \times 3 \times 3$  to  $5 \times 5 \times 5$ . As for CIS, we again see that the randomly shifted mesh provides significantly faster convergence towards the thermodynamic limit. In fact, the  $4 \times 4 \times 4$  and  $5 \times 5 \times 5$  are very similar and suggest semiquantitative convergence, especially at low energies.

In addition to the spectral intensities, the excitation energies also exhibit large finite-size errors. These latter finite-size errors are simpler to remove by extrapolation. Our final EOM-CCSD spectra shown in Fig. 1 have been rigidly shifted by the finite-size error of the first excitation energy. This finite-size error is determined by extrapolation, assuming that the finitesize error decays as  $O(N_k^{-1})$ . Raw data and extrapolation fits are shown in Fig. 3 for four of the solids studied here. We see that the convergence behavior is similar for all four solids, but  $\Gamma$ -centered k-point meshes perform slightly better for indirect materials while randomly shifted meshes perform slightly better for direct gap materials. At the largest k-point meshes, the finite-size errors are in the range of 0.1–0.4 eV. The results in Fig. 2 make it clear that increased Brillouin zone sampling has a complex effect on the spectra and this rigid shift is only an approximation to ensure the correct onset of absorption.

Beyond the finite-size errors, we have studied the effects of

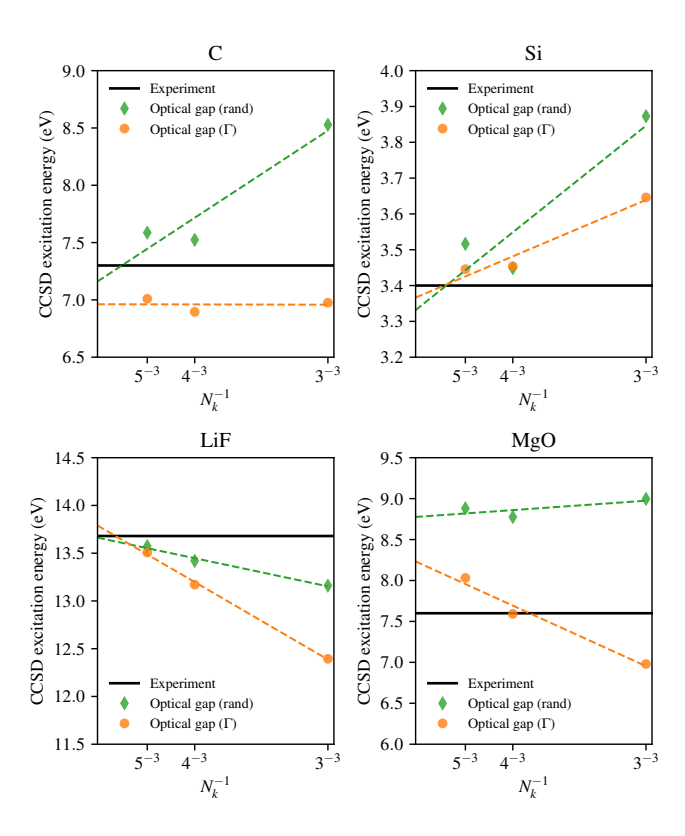


FIG. 3. Extrapolation of first excitation energies to the thermodynamic limit for C, Si, LiF, and MgO. Frozen virtual orbitals and partitioning are used in all cases.

three other approximations: incomplete basis set, frozen orbitals, and the partitioning of EOM-CCSD, as shown in Fig. 4 for diamond with the same randomly-shifted k-point mesh as above. In Fig. 4(a), we show that the basis set incompleteness error is negligible by comparing the spectrum obtained with two types of pseudopotentials, GTH [51, 52] and ccECP [67–70], combined with their corresponding double- and triplezeta basis sets. These calculations were performed with a  $2 \times 2 \times 2$  k-point mesh and without freezing any orbitals. Additionally, we see that the use of two distinct pseudopotentials does not introduce a noticeable difference in the calculated spectra.

In Fig. 4(b), we test the impact of orbital freezing and partitioning by showing four spectra, all performed with a  $3 \times 3 \times 3$  k-point mesh: (1) the EOM-CCSD spectrum without approximations, (2) the EOM-CCSD spectrum with only 4 occupied and 4 virtual orbitals correlated, (3) the partitioned EOM-CCSD spectrum without any frozen orbitals, and (4) the partitioned EOM-CCSD spectrum with 4 occupied and 4 virtual orbitals correlated. We see that freezing orbitals causes a roughly rigid shift of the spectrum to higher energy by about 0.2–0.5 eV. The shift is not perfectly rigid and, as expected, the discrepancy is worst at high energies. In contrast, the partitioning error causes a roughly rigid shift to lower energy by a similar amount. When both approximations are applied, we obtain a spectrum close to the one without approximations due to fortuitous cancellation of error, justifying our use of this af-

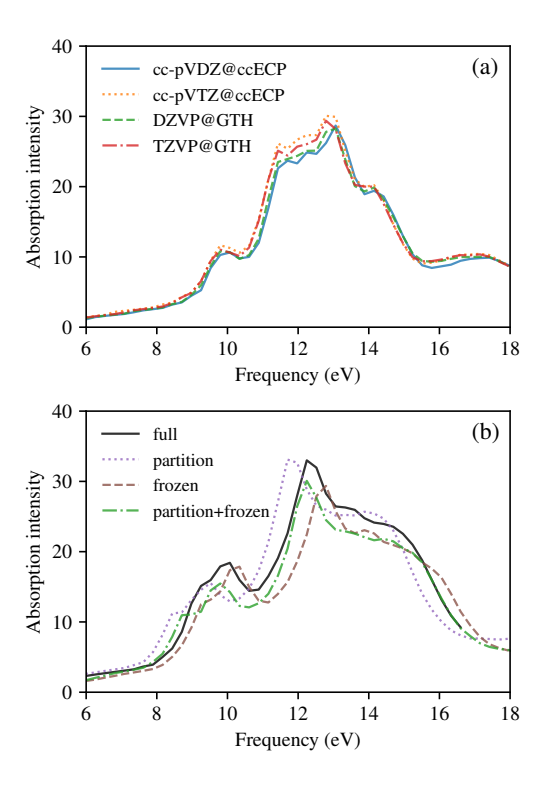


FIG. 4. EOM-CCSD absorption spectra of diamond with various basis sets and approximations as indicated. A random k-point shift and a Lorentzian broadening of  $\eta=0.5$  eV is used in all cases. (a) Comparison of EOM-CCSD spectra (without partitioning and with all orbitals correlated) using four different basis set/pseudopotential combinations as indicated. The Brillouin zone was sampled with a  $2\times2\times2$  k-point mesh. (b) Comparison of the full EOM-CCSD spectra and various approximations as indicated using the DZVP basis set and GTH pseudopotential. The Brillouin zone was sampled with a  $3\times3\times3$  k-point mesh.

fordable approach when scaling up to larger k-point meshes.

The effect of all errors discussed in this subsection can be approximated with a rigid spectral shift according to the error in the first excitation energy. These corrections for both  $\Gamma$ -centered and randomly shifted k-point meshes are summarized in Table I for all six material studied. The base result  $(E_{555})$  is obtained with partitioned EOM-CCSD using frozen orbitals and a  $5 \times 5 \times 5$  k-point mesh. To this, we apply two composite-style corrections:  $\Delta_{TDL}$  is the difference between the excitation energy in the thermodynamic limit obtained by extrapolation and  $E_{555}$ , where all calculations are performed with partitioned EOM-CCSD/DZVP with frozen orbitals, and  $\Delta_{frz+part}$  is the difference between EOM-CCSD without approximations and partitioned EOM-CCSD with frozen orbitals, using a  $3 \times 3 \times 3$  k-point mesh. These two corrections are roughly comparable in magnitude but strongly system dependent. Although each correction alone may shift the energy by up to 0.5 eV, the final correction is typically quite small due to error cancellation. We reiterate that the use of a rigid shift to the entire spectrum is more justified for the frozen orbital and partitioning approximations than it is for finite-size effects and that its accuracy degrades at higher energies.

TABLE I. EOM-CCSD first excitation energies and corrections (in eV) for Si, SiC, C, MgO, BN, and LiF.

	$E_{555}$	$\Delta_{ ext{TDL}}$	$\Delta_{ m frz+part}$	$E_{ m final}$	
		randomly shifted k-point mesh			
Si	3.52	-0.18	0.20	3.53	
SiC	5.83	0.14	0.53	6.50	
C	7.59	-0.43	0.37	7.53	
MgO	8.88	-0.11	0.28	9.05	
BN	11.06	-0.16	0.24	11.14	
LiF	13.57	0.09	-0.06	13.61	
	$\Gamma$ -centered $k$ -point mesh				
Si	3.45	-0.08	-0.12	3.25	
SiC	6.10	-0.28	0.24	6.06	
C	7.01	-0.05	0.29	7.25	
MgO	8.03	0.20	0.41	8.64	
BN	10.82	0.07	0.16	11.06	
LiF	13.51	0.28	0.00	13.79	

To reiterate, the final spectra presented in Fig. 1 were obtained with a  $5 \times 5 \times 5$  k-point mesh using partitioned EOM-CCSD, correlating 4 occupied and 4 virtual orbitals per k-point, and then rigidly shifted according to the corrections given in Tab. I to approximately correct for finite-size errors, frozen orbitals, and the partitioning approximation applied to the dense doubles block of the Hamiltonian.

### V. CONCLUSIONS AND OUTLOOK

We have presented the first absorption spectra of atomistic, three-dimensional solids using an approximation to periodic EOM-CCSD, focusing on Si, SiC, C, MgO, BN, and LiF. With increasing Brillouin zone sampling, we observe no problems associated with the lacking size-extensivity of EOM-CCSD spectral intensities [46, 47]. This may be due to the reasonably complete basis set [48] provided by a solid-state environment, but further study is warranted. After accounting for a

number of sources of error, our best and final spectra show reasonably good agreement with experimental spectra, indicating that EOM-CCSD is a promising and tractable approach for the study of excitations in solids. In many materials, we find that spectral shapes are well reproduced but are shifted to higher energies with respect to experiment by about 1 eV. We attribute this discrepancy to a combination of incomplete electron correlation (i.e., the impact of triple and higher excitations) and the neglect of zero-point and finite-temperature vibrational effects [71–73]. Unlike in TDDFT and GW-BSE, in CCSD there is reduced freedom in the choice of starting point due to its weak sensitivity to the employed reference determinant.

Aside from this shift to higher energies, we see the worst agreement with experiment for small-gap semiconductors that we attribute to the breakdown of the partitioning approximation, which corresponds to a low-order treatment of screening, and to the remaining finite-size errors. Whereas corrections and extrapolations of isolated energies is largely successful, doing the same for spectral intensities is not straightforward. The high cost of EOM-CCSD calculations precludes brute force convergence and future work will explore the use of interpolation [7], twist averaging [74], and double-grid schemes [75], which have been very successful at providing converged GW-BSE spectra at reduced computational cost. With these improvements, we can revisit the accuracy of the partitioning approximation compared to full EOM-CCSD for small-gap semiconductors like silicon.

#### ACKNOWLEDGMENTS

X.W. thanks Alan Lewis for helpful discussion. This work was supported in part by the National Science Foundation under Grant No. OAC-1931321. All calculations were performed using resources provided by the Flatiron Institute. The Flatiron Institute is a division of the Simons Foundation.

<sup>[1]</sup> E. Runge and E. K. U. Gross, Phys. Rev. Lett. **52**, 997 (1984).

<sup>[2]</sup> L. Reining, V. Olevano, A. Rubio, and G. Onida, Phys. Rev. Lett. 88, 066404 (2002).

<sup>[3]</sup> C. A. Ullrich and Z.-h. Yang, "Excitons in time-dependent density-functional theory," in *Density-Functional Methods for Excited States*, edited by N. Ferré, M. Filatov, and M. Huix-Rotllant (Springer International Publishing, Cham, 2016) pp. 185–217.

<sup>[4]</sup> L. J. Sham and T. M. Rice, Phys. Rev. 144, 708 (1966).

<sup>[5]</sup> W. Hanke and L. J. Sham, Phys. Rev. B 21, 4656 (1980).

<sup>[6]</sup> S. Albrecht, L. Reining, R. D. Sole, and G. Onida, Phys. Status Solidi A 170, 189 (1998).

<sup>[7]</sup> M. Rohlfing and S. G. Louie, Phys. Rev. B 62, 4927 (2000).

<sup>[8]</sup> G. Onida, L. Reining, and A. Rubio, Rev. Mod. Phys. **74**, 601

<sup>[9]</sup> F. Bruneval, F. Sottile, V. Olevano, and L. Reining, J Chem Phys 124, 144113 (2006).

<sup>[10]</sup> S. Botti, A. Schindlmayr, R. D. Sole, and L. Reining, Rep. Prog. Phys. 70, 357 (2007).

<sup>[11]</sup> J. Paier, M. Marsman, and G. Kresse, Phys. Rev. B 78, 121201 (2008)

<sup>[12]</sup> A. F. Izmaylov and G. E. Scuseria, J. Chem. Phys. 129, 034101 (2008).

<sup>[13]</sup> D. Wing, J. B. Haber, R. Noff, B. Barker, D. A. Egger, A. Ramasubramaniam, S. G. Louie, J. B. Neaton, and L. Kronik, Phys. Rev. Materials 3, 064603 (2019).

<sup>[14]</sup> A. Tal, P. Liu, G. Kresse, and A. Pasquarello, Phys. Rev. Research 2, 032019 (2020).

<sup>[15]</sup> F. Bruneval, S. M. Hamed, and J. B. Neaton, J. Chem. Phys. 142, 244101 (2015).

<sup>[16]</sup> D. Jacquemin, I. Duchemin, A. Blondel, and X. Blase, J. Chem. Theory Comput. 12, 3969 (2016).

<sup>[17]</sup> D. Jacquemin, I. Duchemin, and X. Blase, J. Phys. Chem. Lett. 8, 1524 (2017).

- [18] X. Gui, C. Holzer, and W. Klopper, J. Chem. Theory Comput. 14, 2127 (2018).
- [19] S. Hirata, I. Grabowski, M. Tobita, and R. J. Bartlett, Chem. Phys. Lett. 345, 475 (2001).
- [20] S. Hirata, R. Podeszwa, M. Tobita, and R. J. Bartlett, J. Chem. Phys. 120, 2581 (2004).
- [21] H. Katagiri, J. Chem. Phys. 122, 224901 (2005).
- [22] A. Grüneis, G. H. Booth, M. Marsman, J. Spencer, A. Alavi, and G. Kresse, J. Chem. Theory Comput. 7, 2780 (2011).
- [23] J. McClain, Q. Sun, G. K.-L. Chan, and T. C. Berkelbach, J. Chem. Theory Comput. 13, 1209 (2017).
- [24] T. Gruber, K. Liao, T. Tsatsoulis, F. Hummel, and A. Grüneis, Phys. Rev. X 8, 021043 (2018).
- [25] I. Y. Zhang and A. Grüneis, Front. Mater. 6 (2019), 10.3389/fmats.2019.00123.
- [26] A. M. Lewis and T. C. Berkelbach, Phys. Rev. Lett. 122, 226402 (2019)
- [27] B. T. G. Lau and T. C. Berkelbach, J. Chem. Phys. 152, 224704 (2020).
- [28] A. M. Lewis and T. C. Berkelbach, J. Phys. Chem. Lett. 11, 2241 (2020).
- [29] X. Wang and T. C. Berkelbach, J. Chem. Theory Comput. 16, 3095 (2020).
- [30] K. Emrich, Nuclear Physics A 351, 379 (1981).
- [31] K. Emrich, Nuclear Physics A 351, 397 (1981).
- [32] H. Koch and P. Jørgensen, J. Chem. Phys. 93, 3333 (1990).
- [33] J. F. Stanton and R. J. Bartlett, J. Chem. Phys. 98, 7029 (1993).
- [34] R. Bartlett and M. Musiał, Rev. Mod. Phys. **79**, 291 (2007).
- [35] A. I. Krylov, Annu. Rev. Phys. Chem. 59, 433 (2008).
- [36] R. J. Bartlett, WIREs Comput. Mol. Sci. **2**, 126 (2012).
- [37] Z. G. Soos and S. Ramasesha, J. Chem. Phys. 90, 1067 (1989).
- [38] T. D. Kühner and S. R. White, Phys. Rev. B 60, 335 (1999).
- [39] J. McClain, J. Lischner, T. Watson, D. A. Matthews, E. Ronca, S. G. Louie, T. C. Berkelbach, and G. K.-L. Chan, Phys. Rev. B 93 (2016), 10.1103/physrevb.93.235139.
- [40] J. E. Hicken and D. W. Zingg, SIAM J. Sci. Comput. 32, 1672 (2010).
- [41] P. Virtanen, R. Gommers, T. E. Oliphant, M. Haberland, T. Reddy, D. Cournapeau, E. Burovski, P. Peterson, W. Weckesser, J. Bright, S. J. van der Walt, M. Brett, J. Wilson, K. J. Millman, N. Mayorov, A. R. J. Nelson, E. Jones, R. Kern, E. Larson, C. J. Carey, İ. Polat, Y. Feng, E. W. Moore, J. VanderPlas, D. Laxalde, J. Perktold, R. Cimrman, I. Henriksen, E. A. Quintero, C. R. Harris, A. M. Archibald, A. H. Ribeiro, F. Pedregosa, P. van Mulbregt, A. Vijaykumar, A. P. Bardelli, A. Rothberg, A. Hilboll, A. Kloeckner, A. Scopatz, A. Lee, A. Rokem, C. N. Woods, C. Fulton, C. Masson, C. Häggström, C. Fitzgerald, D. A. Nicholson, D. R. Hagen, D. V. Pasechnik, E. Olivetti, E. Martin, E. Wieser, F. Silva, F. Lenders, F. Wilhelm, G. Young, G. A. Price, G.-L. Ingold, G. E. Allen, G. R. Lee, H. Audren, I. Probst, J. P. Dietrich, J. Silterra, J. T. Webber, J. Slavič, J. Nothman, J. Buchner, J. Kulick, J. L. Schönberger, J. V. de Miranda Cardoso, J. Reimer, J. Harrington, J. L. C. Rodríguez, J. Nunez-Iglesias, J. Kuczynski, K. Tritz, M. Thoma, M. Newville, M. Kümmerer, M. Bolingbroke, M. Tartre, M. Pak, N. J. Smith, N. Nowaczyk, N. Shebanov, O. Pavlyk, P. A. Brodtkorb, P. Lee, R. T. McGibbon, R. Feldbauer, S. Lewis, S. Tygier, S. Sievert, S. Vigna, S. Peterson, S. More, T. Pudlik, T. Oshima, T. J. Pingel, T. P. Robitaille, T. Spura, T. R. Jones, T. Cera, T. Leslie, T. Zito, T. Krauss, U. Upadhyay, Y. O. Halchenko, and Y. V.-B. and, Nat. Meth-
- [42] M. Nooijen and J. G. Snijders, J. Chem. Phys. 102, 1681 (1995).

ods 17, 261 (2020).

[43] J. F. Stanton and J. Gauss, J. Chem. Phys. **103**, 1064 (1995).

- [44] S. R. Gwaltney, M. Nooijen, and R. J. Bartlett, Chem. Phys. Lett. 248, 189 (1996).
- [45] M. F. Lange and T. C. Berkelbach, J. Chem. Phys. 155, 081101 (2021).
- [46] R. Kobayashi, H. Koch, and P. Jørgensen, Chem. Phys. Lett. 219, 30 (1994).
- [47] H. Koch, R. Kobayashi, A. Sanchez de Merás, and P. Jørgensen, J. Chem. Phys. 100, 4393 (1994).
- [48] M. Caricato, G. W. Trucks, and M. J. Frisch, J. Chem. Phys. 131, 174104 (2009).
- [49] Q. Sun, T. C. Berkelbach, N. S. Blunt, G. H. Booth, S. Guo, Z. Li, J. Liu, J. D. McClain, E. R. Sayfutyarova, S. Sharma, S. Wouters, and G. K.-L. Chan, WIREs Comput. Mol. Sci. 8, e1340 (2018).
- [50] Q. Sun, X. Zhang, S. Banerjee, P. Bao, M. Barbry, N. S. Blunt, N. A. Bogdanov, G. H. Booth, J. Chen, Z.-H. Cui, J. J. Eriksen, Y. Gao, S. Guo, J. Hermann, M. R. Hermes, K. Koh, P. Koval, S. Lehtola, Z. Li, J. Liu, N. Mardirossian, J. D. McClain, M. Motta, B. Mussard, H. Q. Pham, A. Pulkin, W. Purwanto, P. J. Robinson, E. Ronca, E. R. Sayfutyarova, M. Scheurer, H. F. Schurkus, J. E. T. Smith, C. Sun, S.-N. Sun, S. Upadhyay, L. K. Wagner, X. Wang, A. White, J. D. Whitfield, M. J. Williamson, S. Wouters, J. Yang, J. M. Yu, T. Zhu, T. C. Berkelbach, S. Sharma, A. Y. Sokolov, and G. K.-L. Chan, J. Chem. Phys. 153, 024109 (2020).
- [51] S. Goedecker, M. Teter, and J. Hutter, Phys. Rev. B 54, 1703 (1996).
- [52] C. Hartwigsen, S. Goedecker, and J. Hutter, Phys. Rev. B 58, 3641 (1998).
- [53] J. VandeVondele, M. Krack, F. Mohamed, M. Parrinello, T. Chassaing, and J. Hutter, Comput. Phys. Commun. 167, 103 (2005).
- [54] Q. Sun, T. C. Berkelbach, J. D. McClain, and G. K.-L. Chan, J. Chem. Phys. 147, 164119 (2017).
- [55] M. R. Ahmadpour Monazam, K. Hingerl, and P. Puschnig, Phys. Rev. B 88, 075314 (2013).
- [56] P. Lautenschlager, M. Garriga, L. Vina, and M. Cardona, Phys. Rev. B 36, 4821 (1987).
- [57] S. Logothetidis and J. Petalas, J. Appl. Phys. 80, 1768 (1996).
- [58] E. D. Palik, Handbook of Optical Constants of Solids, Vol. 3 (Academic Press, New York, 1998).
- [59] D. M. Roessler and W. C. Walker, Phys. Rev. 159, 733 (1967).
- [60] Y. Osaka, A. Chayahara, H. Yokohama, M. Okamoto, T. Hamada, T. Imura, and M. Fujisawa, in *Materials Science Forum*, Vol. 54-55, edited by J. Pouch and S. Alteroviz (Aedermanndorf, Switzerlad, 1990) pp. 277–294.
- [61] A. Tararan, S. di Sabatino, M. Gatti, T. Taniguchi, K. Watanabe, L. Reining, L. H. G. Tizei, M. Kociak, and A. Zobelli, Phys. Rev. B 98, 094106 (2018).
- [62] M. F. Lange and T. C. Berkelbach, J. Chem. Theory Comput. 14, 4224 (2018).
- [63] T. C. Berkelbach, J. Chem. Phys. 149, 041103 (2018).
- [64] R. Laskowski, N. E. Christensen, G. Santi, and C. Ambrosch-Draxl, Phys. Rev. B 72, 035204 (2005).
- [65] F. Fuchs, C. Rödl, A. Schleife, and F. Bechstedt, Phys. Rev. B 78, 085103 (2008).
- [66] T. Sander, E. Maggio, and G. Kresse, Phys. Rev. B 92, 045209 (2015).
- [67] M. C. Bennett, C. A. Melton, A. Annaberdiyev, G. Wang, L. Shulenburger, and L. Mitas, J. Chem. Phys. 147, 224106 (2017)
- [68] M. C. Bennett, G. Wang, A. Annaberdiyev, C. A. Melton, L. Shulenburger, and L. Mitas, J. Chem. Phys. 149, 104108 (2018).

- [69] A. Annaberdiyev, G. Wang, C. A. Melton, M. C. Bennett, L. Shulenburger, and L. Mitas, J. Chem. Phys. 149, 134108 (2018).
- [70] G. Wang, A. Annaberdiyev, C. A. Melton, M. C. Bennett, L. Shulenburger, and L. Mitas, J. Chem. Phys. 151, 144110 (2019).
- [71] J. Noffsinger, E. Kioupakis, C. G. Van de Walle, S. G. Louie, and M. L. Cohen, Phys. Rev. Lett. 108, 167402 (2012).
- [72] C. E. Patrick and F. Giustino, J. Phys.: Condens. Matter **26**, 365503 (2014).
- [73] W. R. L. Lambrecht, C. Bhandari, and M. van Schilfgaarde, Phys. Rev. Materials 1, 043802 (2017).
- [74] C. Lin, F. H. Zong, and D. M. Ceperley, Phys. Rev. E 64, 016702 (2001).
- [75] D. Kammerlander, S. Botti, M. A. L. Marques, A. Marini, and C. Attaccalite, Phys. Rev. B 86, 125203 (2012).